

# RSC Advances



This is an *Accepted Manuscript*, which has been through the Royal Society of Chemistry peer review process and has been accepted for publication.

*Accepted Manuscripts* are published online shortly after acceptance, before technical editing, formatting and proof reading. Using this free service, authors can make their results available to the community, in citable form, before we publish the edited article. This *Accepted Manuscript* will be replaced by the edited, formatted and paginated article as soon as this is available.

You can find more information about *Accepted Manuscripts* in the [Information for Authors](#).

Please note that technical editing may introduce minor changes to the text and/or graphics, which may alter content. The journal's standard [Terms & Conditions](#) and the [Ethical guidelines](#) still apply. In no event shall the Royal Society of Chemistry be held responsible for any errors or omissions in this *Accepted Manuscript* or any consequences arising from the use of any information it contains.



## RSC Advances

## Paper

IGH5UYD2E Cite this: DOI:  
10.1039/x0xx00000x

Received 00th January 2015,  
Accepted 00th January 2015

DOI: 10.1039/x0xx00000x

[www.rsc.org/](http://www.rsc.org/)

## Copper Supported on MWCNT-Guanidine Acetic Acid@Fe<sub>3</sub>O<sub>4</sub>: Synthesis, Characterization and Application as a Novel Multi-Task Nanocatalyst for Preparation of Triazoles and Bis(indolyl)methanes in Water

Ahmad Shaabani,\* Ronak Afshari, Seyyed Emad Hooshmand, Azadeh Tavousi Tabatabaei and Fatemeh Hajishaabanha

Faculty of Chemistry, Shahid Beheshti University, G. C., P. O. Box 19396-4716, Tehran, Iran Email: [a-shaabani@sbu.ac.ir](mailto:a-shaabani@sbu.ac.ir)  
Electronic supplementary information (ESI) available. See DOI: 10.1039/x0xx00000x

The synthesis of a new supported copper nanocatalyst, with highly dispersed particles, based on magnetic guanidine acetic acid (GAA) functionalized multi-wall carbon nanotube (MWCNT), Cu/MWCNT-GAA@Fe<sub>3</sub>O<sub>4</sub>, has been reported. The synthesized nanocatalyst has been characterized by means of X-ray diffraction (XRD), scanning electron microscopy (SEM), transmission electron microscopy (TEM), energy dispersive X-ray (EDX), elemental analysis (CHN), thermogravimetric analyses (TGA) and Fourier transform infrared (FT-IR). The catalytic activity of Cu/MWCNT-GAA@Fe<sub>3</sub>O<sub>4</sub> was investigated in 1,3-dipolar cycloaddition and condensation reactions in water. The results show a wide ranges of 1,2,3-triazoles and bis(indolyl)methanes have been synthesized in good to excellent yields in a short time. The nanocatalyst can be recovered by applying an external magnetic field which results in easy separation of the catalyst without filtration and reused for several runs without loss of its significant activity.

**Keywords:** Copper nanoparticles, Multi-wall carbon nanotube, Guanidine acetic acid, Click chemistry, Bis(indolyl)methane, Nanocatalyst

## Introduction

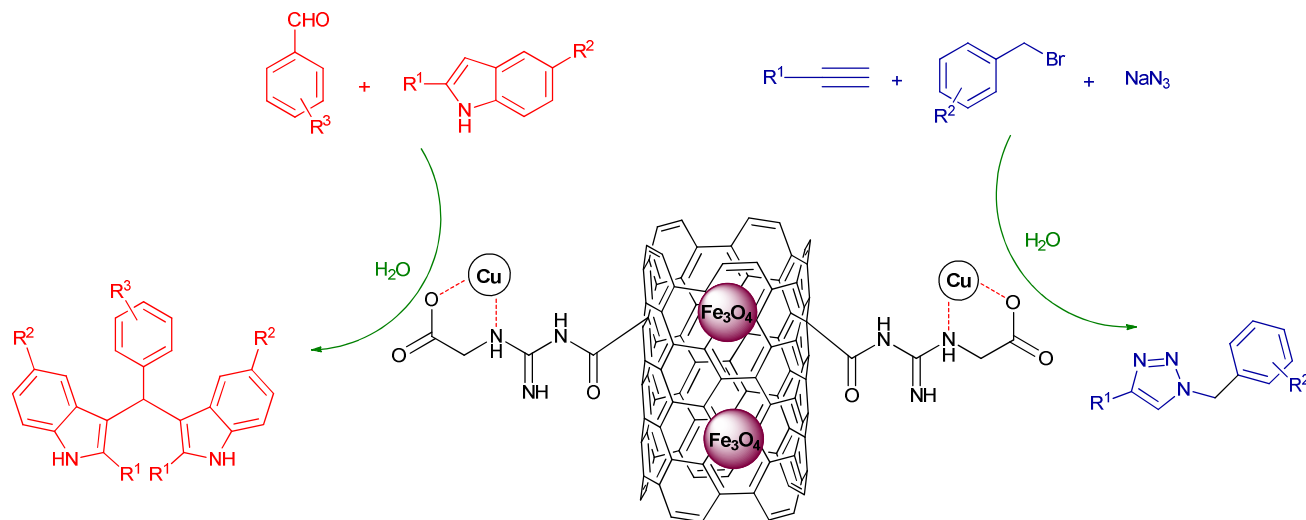
Carbon materials such as carbon nanotubes (CNTs) and graphene oxides (GOs) demonstrate great capabilities to serve as promising substitutes for conventional catalyst supports owing to their large surface area and outstanding electronic conductivity.<sup>1-4</sup> Besides, catalysis by metal based nanocomposites is a powerful method of accelerating a large number of organic reactions. Very recently, the heterogenization of metals onto a support constitutes gained increasing attention in the context of the development of sustainable organometallic chemistry.<sup>5</sup> In this regard, CNTs are one of the main selections for the preparation of multi-task heterogeneous metallic-based catalysts which are a novel class of catalysts able to be involved in at least two consecutive reactions having a different mechanism due to their considerable advantages. However the limited solubility of CNTs has severely impacted their use therefore, functionalization must be developed for improving their solubility, efficiently introducing chemically active sites for use in catalytic reactions and also acting as anchoring sites for deposition of metal nanoparticles.<sup>6, 7</sup> Nowadays, the most promising materials for functionalization of CNTs are polymers such as DNA/RNA,<sup>8</sup> poly porphyrin<sup>9</sup> and chitosan<sup>10, 11</sup> that can decorate CNTs surface to ameliorate their insolubility. Moreover,

immobilized magnetic molecular complexes or nanoparticles onto a support can be recovered from the reaction mixture by an external magnet and their recovery and reuse are additional beneficial attributes.<sup>12</sup> Additionally, the nm size range of these particles facilitates the catalysis process, as an increased surface area is available for the reactions.<sup>13</sup>

The vast majority of the novel heterogeneous catalysts are based on CNT supports, due to the fact that organic groups can be robustly anchored to the CNT surface to provide catalytic centers *via* metal-ligand cooperation. Among the variety of catalytically active metal complexes the transition metals bearing N, O-donor ligands are of great interest and several works have been devoted to consider their catalytic activity in various catalytic organic reactions.<sup>14, 15</sup> One of this N, O-donor ligands is guanidine acetic acid. Guanidine acetic acid (GAA), the essential precursor of creatine, belongs to the class of guanidino compounds which are characterized by the presence of a basic guanidino group,  $\text{HN}=\text{C}(\text{NH}_2)\text{-NH-}$ . Due to the unique properties,<sup>16</sup> this amino acid is involved in many important biological processes, such as creatine deficiency,<sup>17</sup> renal metabolism,<sup>18</sup> thyroid dysfunction,<sup>19</sup> epileptic seizures, hepatic encephalopathy and insulin regulation.<sup>18</sup> Also, the complexation of GAA with Cu(II) for its role in superoxide dismutase was studied.<sup>20</sup> Therefore, guanidine acetic acid with the N, O-donor's ability as a bifunctional ligand can create a novel class of heterogeneous catalyst that can have sufficient properties.

As "point and shoot" coupling tools, click reactions are charming to researchers since its birth,<sup>21</sup> and have been widely used in many hot research fields. However, because of the high activation energy, these cycloadditions generally require high temperatures and long reaction times and usually afford a mixture of the 1,4- and 1,5-regioisomers. The copper catalysts could facilitate the cycloaddition in a regiospecific manner to give only 1,4-disubstituted triazoles and it was reported by Sharpless.<sup>22</sup> This reaction has been reported using the catalysts in the form of Cu(I) salts,<sup>23</sup>  $\text{CuSO}_4$ -ascorbate system,<sup>24</sup> immobilized Cu(I) onto polymers,<sup>25</sup> copper nanoparticles,<sup>26</sup> and nanostructured copper oxide.<sup>27</sup> Therefore, we inferred heterogeneous magnetic Cu/MWCNT catalyst system, in the presence of guanidine acetic acid as the ligand, Cu/MWCNT-GAA@ $\text{Fe}_3\text{O}_4$ , could catalyze this reaction and give rise to click chemistry. Further, for investigating the multi-task capability of a new synthesized nanocatalyst, there catalytic activity has been examined in condensation reaction and interestingly has also been found to be an efficient and reliable catalyst for the facile synthesis of bis(indolyl)methanes in water which constitutes an active area of investigation in pharmaceutical and organic synthesis. Bis(indolyl)methanes, which contain two indole units in a molecule, were found in various natural products possessing important biological activity<sup>28, 29</sup> and as an important component has diverse pharmaceutical properties.<sup>30, 31</sup> One of the most applied procedures for synthesis of bis(indolyl)methanes is based on the electrophilic substitution reaction of indoles with various aldehydes and ketones in the presence of heterogeneous and homogeneous acid catalysts.<sup>32-36</sup>

As part of our ongoing program related to the developing new heterogeneous catalysts for organic transformations,<sup>37-40</sup> and based on our previous investigations on graphene,<sup>41-45</sup> herein we report the synthesis and characterize a new supported copper nanocatalyst on magnetic guanidine acetic acid (GAA) functionalized multi-wall carbon nanotube (MWCNT), Cu/MWCNT-GAA@ $\text{Fe}_3\text{O}_4$ . The as-prepared nanocatalyst showed a high catalytic activity towards azide-alkyne 1,3-dipolar cycloaddition reactions for the synthesis of 1,2,3-triazoles and condensation reaction for the synthesis of bis(indolyl)methanes in the presence of water as a green solvent, yielding catalytic efficiency over several cycles. (Scheme 1).



**Scheme 1.** Synthesis of 1,2,3 triazole and bis(indolyl)methane derivatives by Cu/MWCNT-GAA@Fe<sub>3</sub>O<sub>4</sub> catalyst

## Materials and methods

### 1. General

The materials were purchased from Merck and Aldrich and used without further purification. Carboxyl multi wall carbon nanotubes (purity > 95 %, -COOH content: 2.00 wt%, outer diameter: 10-20 nm, inner diameter: 5-10 nm, length: 30 μm, special surface area: 220 m<sup>2</sup> /g) was purchased from Atoor Sanat Abtin, Tehran, Iran. Products were analyzed using a Varian 3900 GC. X-ray diffraction (XRD) pattern of catalyst was recorded on a STOE STADI P with scintillation detector, secondary monochromator using Cu Kα radiation (λ = 0.1540 nm). Copper(II) determination was carried out on an FAAS (Shimadzu model AA-680 flame atomic absorption spectrometer) with a Cu hollow cathode lamp at 324.7 nm, using an air-acetylene flame. Transmission Electron Microscopy (TEM) was performed using a transmission microscope Philips CM-30 with an accelerating voltage of 150 Kv. Scanning electron microscopy (SEM) observations were carried out on an electron microscopy Philips XL-30 ESEM. Thermogravimetric analysis (TGA) was carried out using STA 1500 instrument at a heating rate of 10 °C min<sup>-1</sup> in air. Melting points were measured on an Electrothermal 9100 apparatus and are uncorrected. IR spectra were recorded on a Shimadzu IR-470 spectrometer. The elemental analyses were performed with an Elementar Analysensysteme GmbH VarioEL. <sup>1</sup>H and <sup>13</sup>C NMR spectra were recorded on a BRUKER DRX-300 AVANCE spectrometer at 300.13 and 75.47 MHz. NMR spectra were obtained in DMSO-d<sub>6</sub> and CDCl<sub>3</sub>.

### 1 Preparation of catalyst

#### 2.1 Preparation of MWCNT-COCl

The carboxylic acid group of MWCNT-COOH was converted to formyl chloride *via* reaction with thionyl chloride. In a round bottom flask, an excess amount of SOCl<sub>2</sub> (30 ml) was added to MWCNT-COOH (0.100 g). The suspension was refluxed for 48 h at 75 °C. Thereafter, the sample was evaporated under reduced pressure, followed by a complete removal of unreacted SOCl<sub>2</sub> on a rotary evaporator with a vacuum pump. The remaining solid (MWCNT-COCl) was washed out three times with anhydrous tetrahydrofuran (THF) and dried in an oven at 60 °C for 5 h.

#### 2.2 Preparation of MWCNT-GAA

In a typical procedure, 0.080 g MWCNT-COCl was dispersed in 25 ml DMF and sonicated for 30 min then mixed with 0.060 g (0.001 mol) GAA. The mixture was stirred for 5 h under N<sub>2</sub> atmosphere at room temperature. Then the solvent was evaporated, remaining solid washed with acetone and the precipitate dried in vacuum at 60 °C to afford MWCNT-GAA.

### 2.3 Preparation of Cu/MWCNT-GAA

MWCNT-GAA (0.500 g) was dispersed in water, CuCl<sub>2</sub> · 2H<sub>2</sub>O (0.043 g, 0.00025 mmol) which was dissolved in 5 ml water added dropwise, then ascorbic acid (50 mL, 0.025M) was added, temperature of mixture was increased to 80 °C and stirring continued at 80 °C for 24 h. The solvent was evaporated, and the remaining solid was washed three times with deionized water and ethanol. Finally the precipitate was dried in vacuum at 60 °C overnight to give Cu/MWCNT-GAA.

### 2.4 In situ preparation of Cu/MWCNT-GAA@Fe<sub>3</sub>O<sub>4</sub>

The next step in the accomplishment of catalyst preparation was synthesis of the magnetic Fe<sub>3</sub>O<sub>4</sub> using co-precipitation technique.<sup>46</sup> The Fe<sub>3</sub>O<sub>4</sub> NPs (1.000 g) was dispersed in water (15 mL) and sonicated for 15 min then MWCNT-GAA (1.000 g) added and sonication continued for 2 h at room temperature. Then, a solution of CuCl<sub>2</sub> · 2H<sub>2</sub>O (0.043 g, 0.00025 mmol) in 5 mL water was added dropwise to the reaction mixture, followed by addition of ascorbic acid (50 mL, 0.025M). The reaction mixture was stirred on magnetic heater stirrer at 80 °C for 24 h. Finally, by applying an external magnet, Cu/MWCNT-GAA@Fe<sub>3</sub>O<sub>4</sub> nanoparticles were collected and washed three times with deionized water/ethanol and the magnetic precipitate was dried in vacuum at 60 °C.

### 3. General procedure for the synthesis of 1,2,3-triazoles

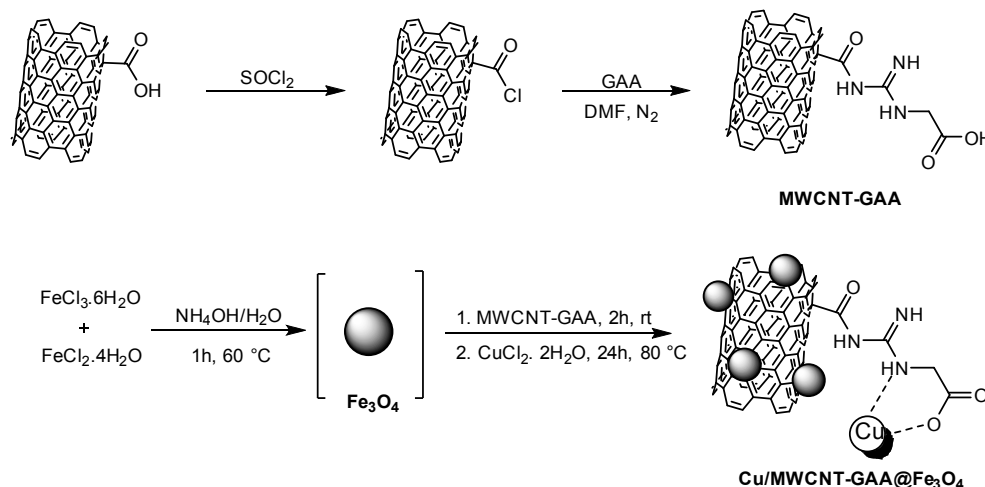
Alkynes (1 mmol), benzyl bromide derivatives (1 mmol) and sodium azide (1 mmol, 0.065 g) were added to a 10 ml round bottom flask fitted with a magnetic stirrer containing a suspension of catalyst (0.400 mol%, 0.020 g) in water (5 mL). The resultant mixture was heated at 50 °C. The progress of the reaction was followed by thin layer chromatography (TLC) (ethyl acetate/n-hexane). Upon completion, the mixture cooled to room temperature and the catalyst separated using an external magnet and the product was extracted with chloroform. The solvent was removed in vacuum to afford the pure product. If necessary the purification was performed by recrystallization from ethyl acetate or ethanol.

### 4. General procedure for the synthesis of bis(indolyl)methanes

In a 10 mL round bottom flask equipped with magnetic stir bar an indole (1 mmol), an aldehyde (0.5 mmol) and water (5 mL) were added. The catalyst (0.200 mol%, 0.01 g) was added and the mixture was stirred at 70 °C for 40-80 min. Progress of reaction was monitored by TLC (ethyl acetate/n-hexane). Then chloroform (2 × 5 mL) was added to the reaction mixture and the catalyst was separated using an external magnet. The chloroform layer was separated, evaporated under reduced pressure to give the crude product which was purified *via* recrystallization in ethanol–water mixture.

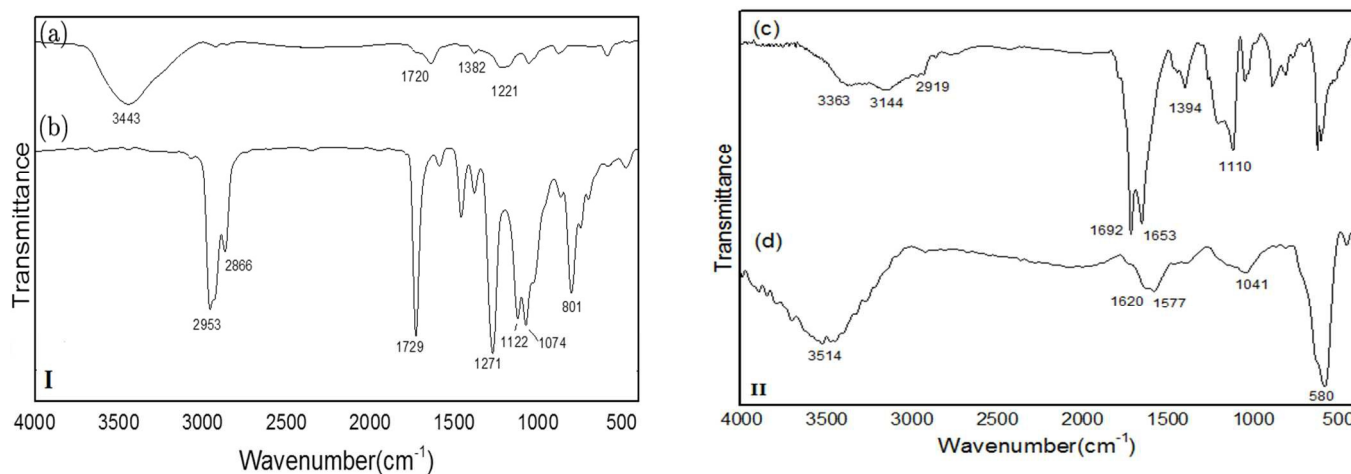
### Results and discussion

Through the synthesis of the novel catalyst, Cu nanoparticles has been anchored to the side walls of MWCNT *via* guanidine acetic acid as a linker.<sup>47</sup> The schematic pathway for preparation of Cu/MWCNT-GAA@Fe<sub>3</sub>O<sub>4</sub> is shown in Scheme 2.



**Scheme 2.** Preparation steps for fabricating heterogeneous Cu/MWCNT-GAA@Fe<sub>3</sub>O<sub>4</sub> nanocomposite

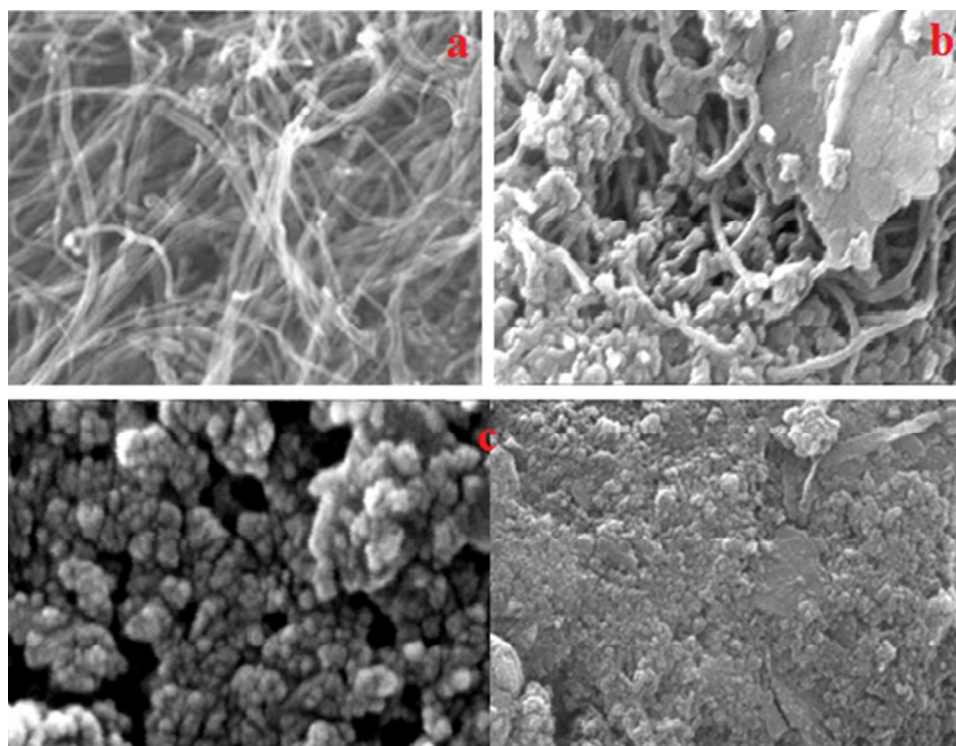
Cu/MWCNT-GAA@Fe<sub>3</sub>O<sub>4</sub> was prepared by chemical functionalization of MWCNT with guanidine acetic acid and the GAA content in the nanocatalyst was calculated to be 2.62 mmol/g, according to the nitrogen content measured by CHN. The FAAS method was used for determining Cu content of the nanocatalyst and the weight percentage of Cu was determined 1.2%. FT-IR spectra of the MWCNT-COOH, MWCNT-COCl, MWCNT-GAA and Cu/MWCNT-GAA@Fe<sub>3</sub>O<sub>4</sub> are shown in Fig. 1. FT-IR peaks for MWCNT-COOH show a broad peak at 3443 cm<sup>-1</sup> due to the stretching vibration of -OH bond, 1720 cm<sup>-1</sup> peak attributed to the presence of carbonyl groups and peak at 1382 cm<sup>-1</sup> corresponds to O-H bond in carboxylic group. A peak at 1221 cm<sup>-1</sup> is assigned to C-O bond stretching (Fig. 1, I-a). FT-IR spectra of MWCNT-COCl confirmed the conversion of C-OH groups to C-Cl by the absence of broad peak of -OH and presence of sharp peak at 801 cm<sup>-1</sup> which indicated C-Cl bonding and the slight shift in the C=O stretching to 1729 cm<sup>-1</sup> (Fig. 1, I-b). Immobilization of the GAA on the MWCNT-COCl can be inferred from FT-IR spectroscopy (Fig. 1, II -c). As a result, the carboxylic bonds of CNT have been converted into amide bonds (NH-C=O). The interaction is noticed by the disappearance of C-Cl peak and appearance of C-N stretching at 1394 cm<sup>-1</sup>. In addition, the FT-IR spectrum of MWCNT-GAA has some bands at 3363, 2935 and 1692 cm<sup>-1</sup> corresponded to the N-H, C-H, C=O stretches respectively which did not observe for CNT. Finally, FT-IR spectrum of Cu/MWCNT-GAA@Fe<sub>3</sub>O<sub>4</sub> exhibits a broad band at 580 cm<sup>-1</sup> corresponding to the stretching vibration of the Fe-O bonds which is assigned to the spinel form of iron oxide (Fe<sub>3</sub>O<sub>4</sub>).<sup>48</sup> The slight shift in the C=O stretching bonds to 1620 and 1577 cm<sup>-1</sup> may be due to the chelation of Cu nanoparticles on the surface of MWCNT-GAA@Fe<sub>3</sub>O<sub>4</sub> (Fig. 1, II -d).



**Fig. 1** FT-IR spectra of: (I-a) MWCNT-COOH; (I-b) MWCNT-COCl; (II-c) MWCNT-GAA and (II-d) Cu/MWCNT-GAA@Fe<sub>3</sub>O<sub>4</sub>



Selected images of scanning electron microscopy (SEM) and transmission electron microscopy (TEM) have been used to study the structure and morphology of the catalyst. The SEM and TEM images of MWCNT-COCl show the nanotube structure of this particle with low dispersity (Fig. 2a and d). Shape and structure of MWCNTs were constantly remained after functionalization with GAA and caused the higher dispersion of nanotubes (Fig. 2e). After functionalization of the MWCNT-COCl *via* GAA and immobilization of Cu and Fe<sub>3</sub>O<sub>4</sub> NPs, the ligand and immobilized NPs can act as an obstacle in agglomeration of nanocatalyst so it could be used as a suitable catalyst for any reaction. To confirm the formation of Cu nanoparticles through the preparation of nanocatalyst, the Cu/MWCNT-GAA has been synthesized by similar procedure in the absence of Fe<sup>2+</sup> and Fe<sup>3+</sup>. The white dots represent anchored Cu NPs, having a spherical-like shape, with a diameter of ~20 nm that dispersed over the side walls of MWCNT-GAA which directly visualized by SEM and TEM images (Fig. 2, b and f). The SEM and TEM images of Cu/MWCNT-GAA@Fe<sub>3</sub>O<sub>4</sub> show that Fe<sub>3</sub>O<sub>4</sub> NPs are well incorporated on the surface of Cu/MWCNT-GAA with semi-spherical morphology. Also, Cu NPs can easily be recognized as it appears brighter than Fe<sub>3</sub>O<sub>4</sub> NPs in the TEM (Fig. 2, c and g). The nanoparticles attached to the side walls of the MWCNT-GAA with an average size in the range of 8-25 nm related to Fe<sub>3</sub>O<sub>4</sub> and Cu NPs, respectively. The components of Cu/MWCNT-GAA and Cu/MWCNT-GAA@Fe<sub>3</sub>O<sub>4</sub> were analysed by using an energy dispersive spectrometer. The EDX spectrum shows the elemental composition (Cu) of Cu/MWCNT-GAA (Fig. 2h) and (O, Fe and Cu) of Cu/MWCNT-GAA@Fe<sub>3</sub>O<sub>4</sub> (Fig. 2i).



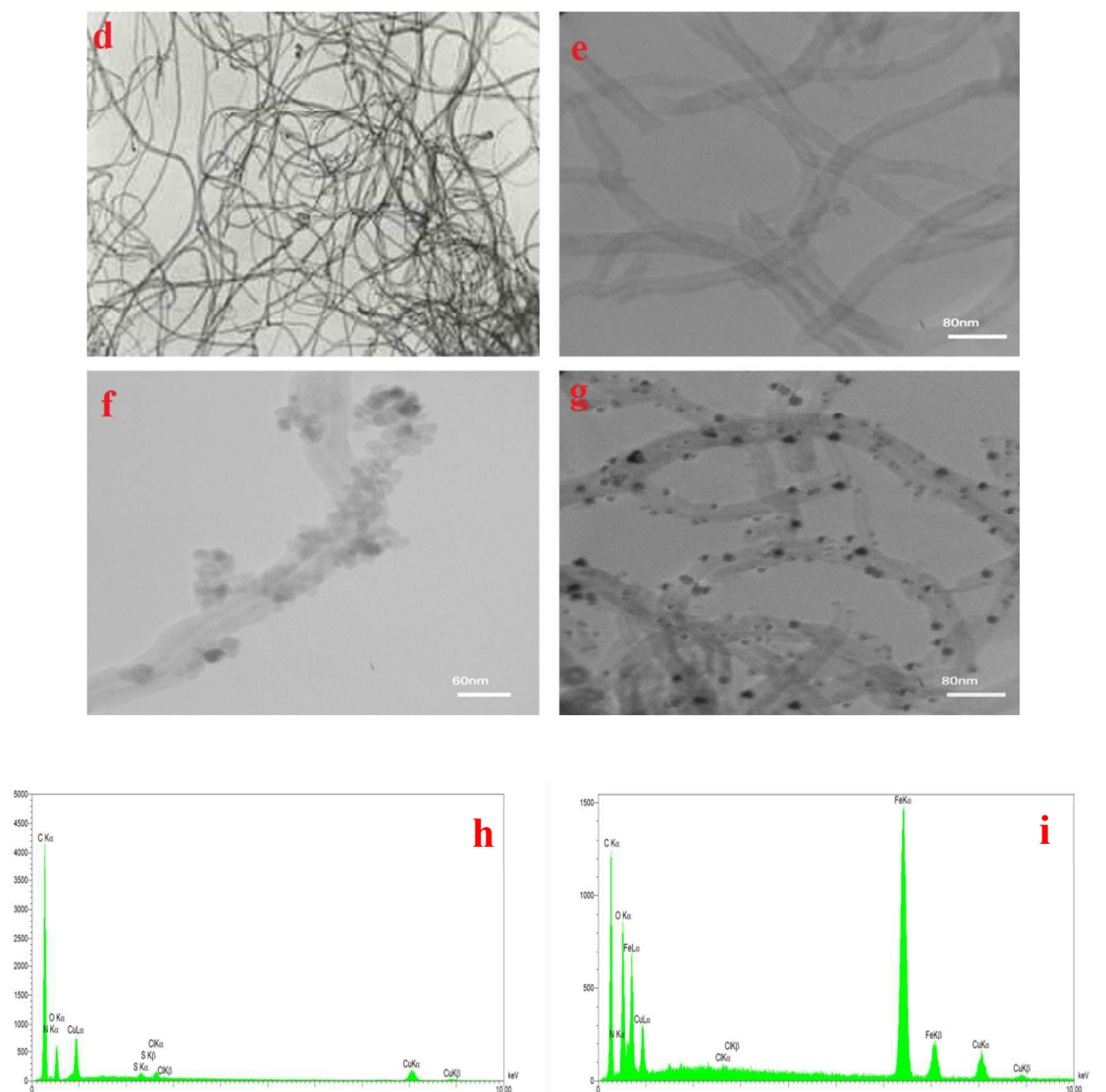


**Fig. 2** SEM images of: (a) MWCNT-COCl. (b) Cu/MWCNT-GAA. (c) Cu/MWCNT-GAA@Fe<sub>3</sub>O<sub>4</sub>. TEM images of: (d) MWCNT-COCl (e) MWCNT-GAA (f) Cu/MWCNT-GAA (g) Cu/MWCNT-GAA@Fe<sub>3</sub>O<sub>4</sub>. EDXS spectrum of: (h) Cu/MWCNT-GAA (i) Cu/MWCNT-GAA@Fe<sub>3</sub>O<sub>4</sub>

The XRD patterns of MWCNT-COCl, MWCNT-GAA and Cu/MWCNT-GAA@Fe<sub>3</sub>O<sub>4</sub> are shown in Fig. 3. The diffraction peaks at  $2\theta = 25.53^\circ$ ,  $42.28^\circ$  were associated with the (002), (100) corresponding to the hexagonal graphite structure of MWCNT that were appeared in all patterns. In the case of MWCNT-GAA there is no obvious change in the structure of MWCNT after functionalization with GAA. After formation of Cu and Fe<sub>3</sub>O<sub>4</sub> NPs onto the surface of functionalized MWCNT, the pattern shows the new peaks. The peaks at  $43.3^\circ$ ,  $50.26^\circ$  and  $74.56^\circ$  were assigned with the (111), (200) and (220) demonstrating the formation of Cu NPs<sup>49</sup> also  $30.87^\circ$ ,  $35.30^\circ$ ,  $42.93^\circ$ ,  $53.35^\circ$ ,  $57.00^\circ$ , and  $62.66^\circ$  peaks corresponding to the (220), (311), (400), (422), (511), and (440) was obtained due to the cubic spinel structure of Fe<sub>3</sub>O<sub>4</sub> NPs.<sup>50</sup> In brief, this XRD patterns show that the structure of MWCNT support was uniformly maintained through the reaction process also, Cu and Fe<sub>3</sub>O<sub>4</sub> NPs were formed successfully.



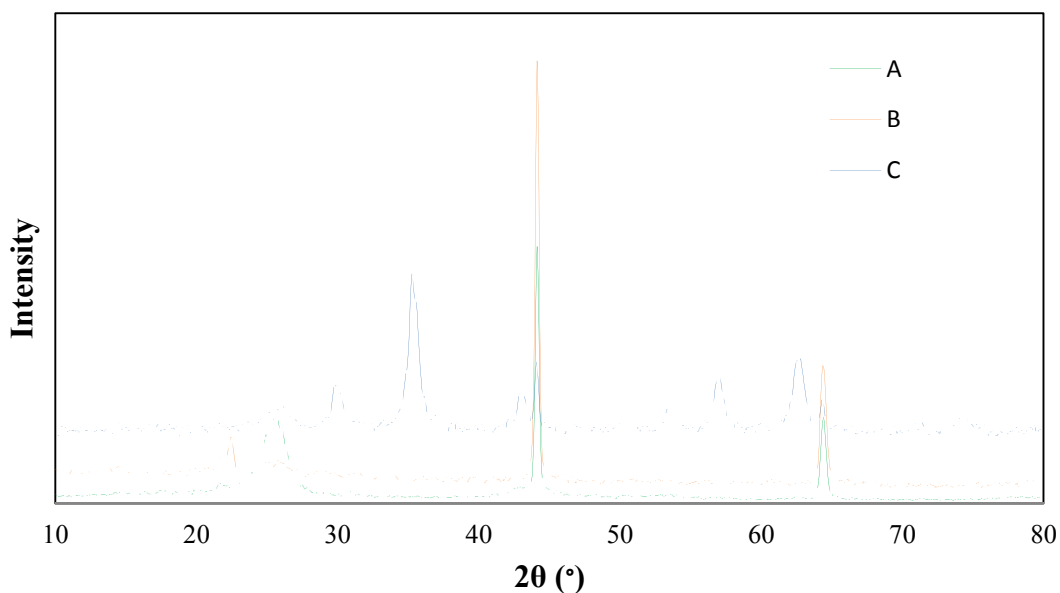


**Fig. 3** XRD patterns of MWCNT-COCl (A), MWCNT-GAA (B), and Cu/MWCNT-GAA@Fe<sub>3</sub>O<sub>4</sub> (C).

In order to obtain information on the thermal stability, TGA experiments are carried out by heating MWCNT-COOH, MWCNT-GAA and Cu/MWCNT-GAA@Fe<sub>3</sub>O<sub>4</sub> up to 700 °C under air at a heating rate of 10 °C/min (Fig. 4). The TGA curves showed the initial weight loss up to 200 °C due to the removal of moisture and physically adsorbed solvent. In the TGA curve of the MWCNT-COOH a second weight loss occurred between 550-700 °C, which related to the oxidation of the purified MWCNTs. The MWCNT-GAA showed same initial weight loss and two new stages appeared for weight loss consisting of deformation of functional groups and decomposition of organic linker along by MWCNTs oxidation in the range of 220-550 and 550-700 °C, respectively. However, in the case of Cu/MWCNT-GAA@Fe<sub>3</sub>O<sub>4</sub> clearly observed three temperature ranges of initial weight diminution same as the previous case with difference in amounts of weight losses. The residual weight of MWCNT-COOH, MWCNT-GAA and Cu/MWCNT-GAA@Fe<sub>3</sub>O<sub>4</sub> were 62%, 17% and 58%, respectively. Decreases the amounts of residual weight of MWCNT-GAA compared to MWCNT-COOH related to the tethered of GAA to MWCNT. The amounts of the GAA attached to MWCNT can be calculated from the difference in weight loss of the MWCNT-COOH and MWCNT-GAA hybrids and is 50 wt% at 700 °C. However, the residual weight of Cu/MWCNT-GAA@Fe<sub>3</sub>O<sub>4</sub> confirmed the addition of Cu and Fe<sub>3</sub>O<sub>4</sub> NPs to the recent functionalized nanocomposite.

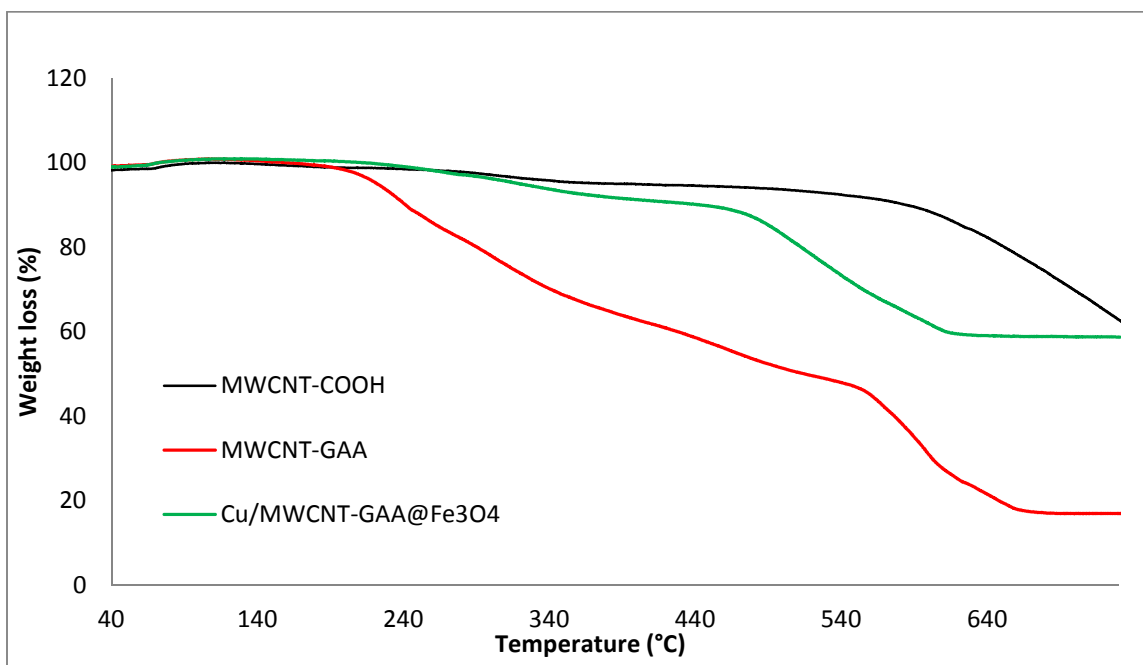
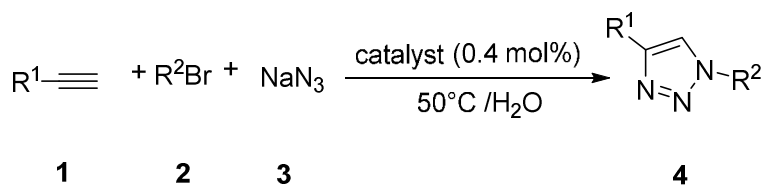


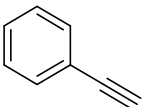
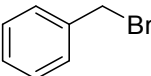
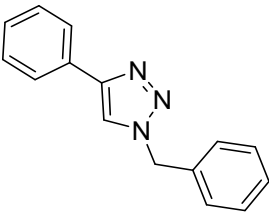
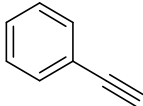
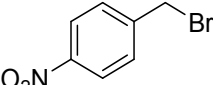
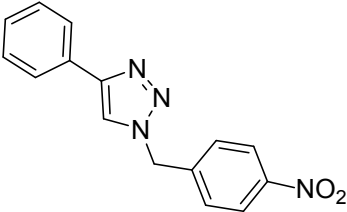
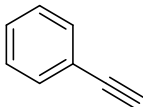
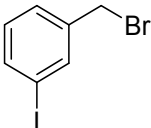
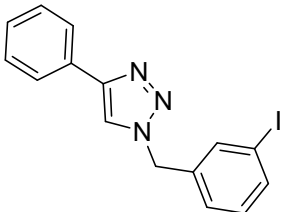
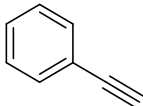
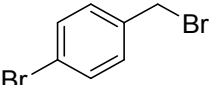
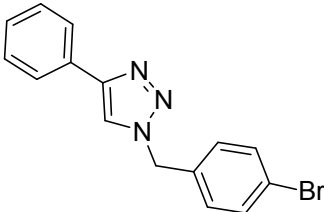
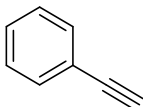
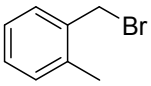
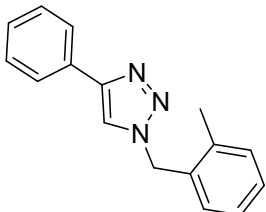
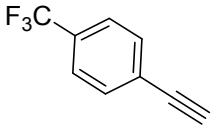
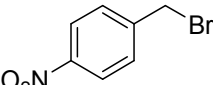
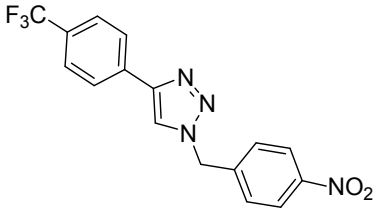
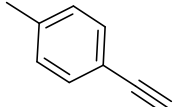
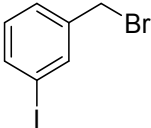
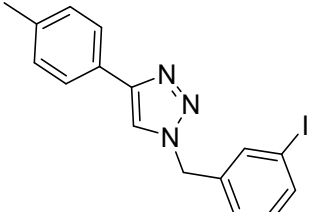
Fig. 4 TG curves recorded in air at a heating rate of 10 °C/min

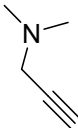
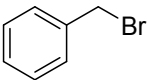
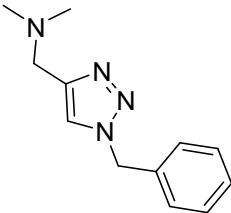
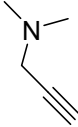
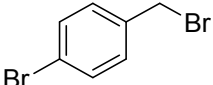
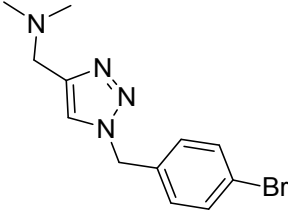
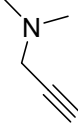
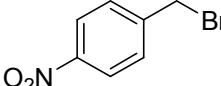
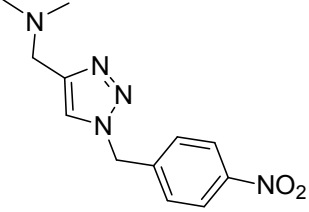
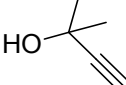
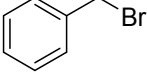
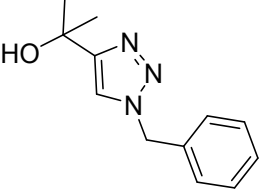
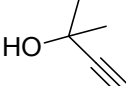
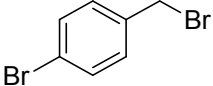
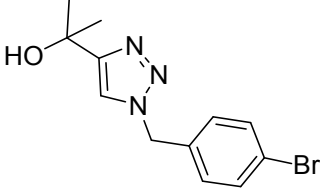
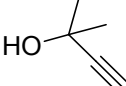
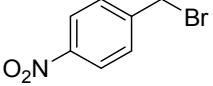
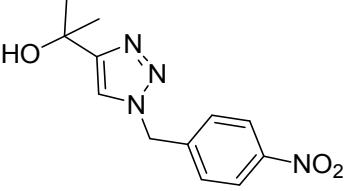
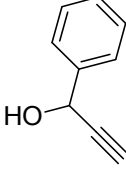
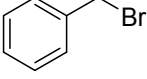
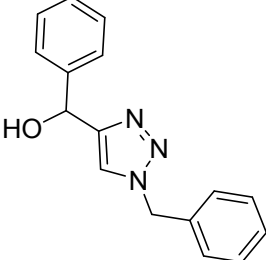
To show the efficiency of the newly synthesized nanocatalyst, the catalytic activity of Cu/MWCNT-GAA@Fe<sub>3</sub>O<sub>4</sub> was evaluated in a click reaction for the synthesis of substituted 1,2,3-triazoles. These triazole compounds are the most important heterocycles, owing to their unique chemical and structural properties and various synthetic methods have been developed for their construction.<sup>51</sup> Recently, the applications of this building block have been extended into various research fields, such as biological science,<sup>52</sup> material chemistry<sup>53</sup> and medicinal chemistry.<sup>54</sup> Our investigation began with the evaluation of Cu/MWCNT-GAA@Fe<sub>3</sub>O<sub>4</sub> as a heterogeneous catalyst in the reaction of phenylacetylene (1 mmol, 0.102 ml), benzyl bromide (1 mmol, 0.118 ml) and sodium azide (1 mmol, 0.065 g) as a model reaction. It was found that a yield of 99 % of the cycloaddition product, 1-benzyl-4-phenyl-1H-1,2,3- triazole, has been obtained for the coupling between benzyl bromide and phenylacetylene (Table 1, entry 1). Then, we explored the versatility of the catalyst for the 1,3-dipolar cycloaddition of structurally diverse benzyl bromides and alkynes, and the results are summarized in Tables 1. All the substrates produced the expected cycloaddition product in water with very good to excellent yields.

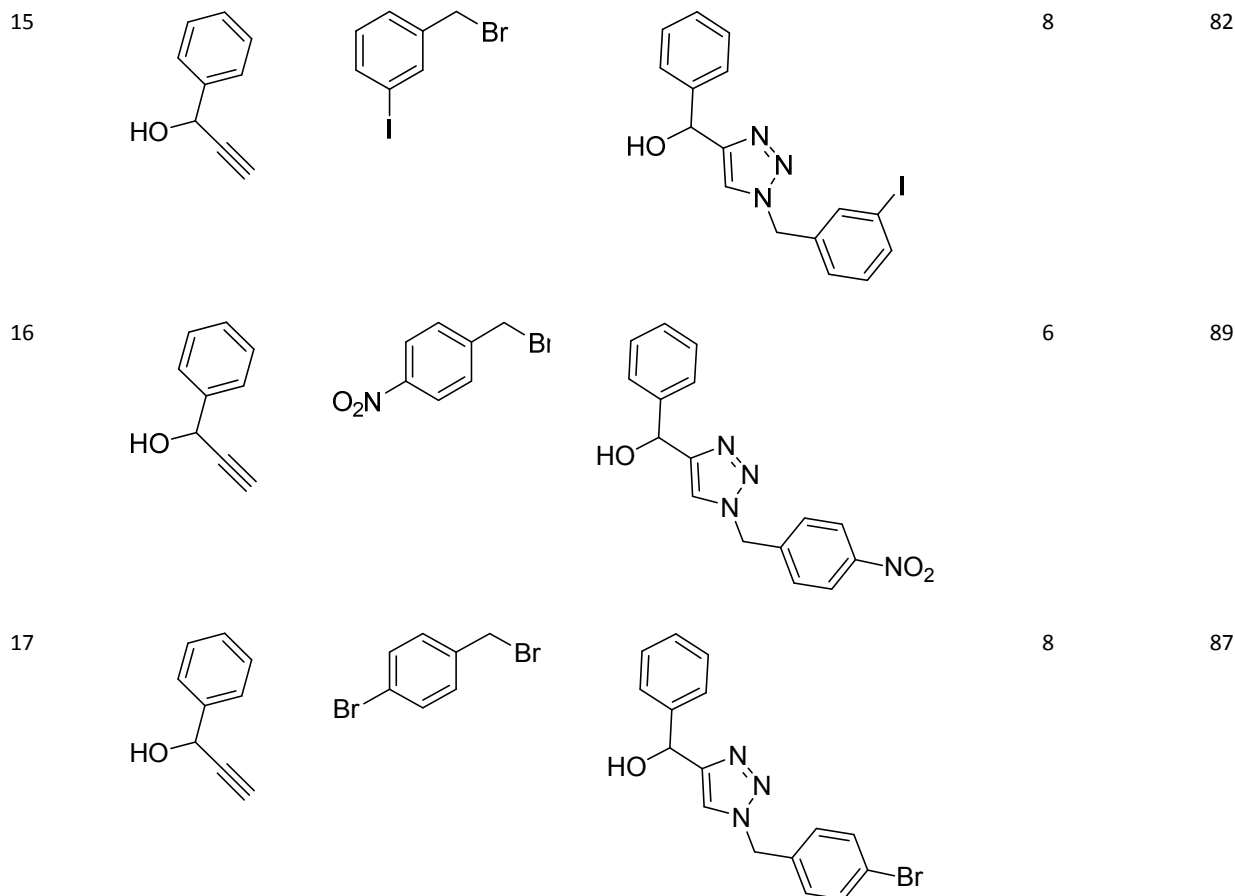


**Table 1.** Three-component 1,3-dipolar azide–alkyne cycloaddition catalysed by Cu/MWCNT-GAA@Fe<sub>3</sub>O<sub>4</sub> using organic halides as the azide precursors<sup>a</sup>

Entry	1	2	Triazoles	Time/h	Yield (%) <sup>b</sup>
-------	---	---	-----------	--------	------------------------

1				1	99
2				2	95
3				2	89
4				2	90
5				2	86
6				2	100
7				3	92

8				7	89
9				8	92
10				8	92
11				9	93
12				10	89
13				8	93
14				7	86



<sup>a</sup>The reaction was carried out using 1 (1mmol) and 2 (1 mmol) and 3 (1 mmol) in the presence of catalyst (0.020 g) at 50 °C, <sup>b</sup>Isolated yield

It is well known that water is considered as a green solvent for various chemical and biological reactions, by considering both an economic and an environmental aspect also during the course of our studies toward the development of new routes to the synthesis of organic compounds using water as a green medium,<sup>55-58</sup> it was decided to use water as an environment friendly solvent. The results show that the click reaction successfully carried out in water with good to excellent yield. As a result, there was no need to solvent optimization.

The efficiency of the synthesized catalyst in comparison with other reported catalysts is given in Table 2. The results show, in the case of Cu/MWCNT-GAA@Fe<sub>3</sub>O<sub>4</sub>, the reaction yield is increased at the relatively shorter reaction times. The better rate of this reaction could be translated due to high surface area and suitable interaction of nanocomposite with substrates by the electrostatic and dipole-dipole interactions. Additionally, interactions between d-orbital of metal and n electron of unsaturated linker and MWCNT can effect on the delocalization of the electron density over both metal and unsaturated structures of nanocomposite. This might be affected on the electrochemical activity of Cu NPs. These data thus show that the Cu NPs activity is significantly enhanced in the presence of magnetic MWCNT. Therefore, this metallic nanocomposite catalysed click reaction in excellent yields under mild thermal conditions in water.

**Table 2.** Comparison of literature catalysts and this work for the synthesis of 1-benzyl-4-phenyl-1H-1,2,3- triazole.

Entry	Catalyst	Reaction conditions	Time (h)	Yield (%)	Ref.
-------	----------	---------------------	----------	-----------	------

1	PVP coated Cu–Fe <sub>3</sub> O <sub>4</sub> NPs	<i>t</i> -BuOH:H <sub>2</sub> O(1:3)/r.t.	3	55	59
2	Cu- <i>p</i> ABA	H <sub>2</sub> O/r.t.	3	97	60
3	Cu@Fe NPs	H <sub>2</sub> O/r.t.	12	93	61
4	SiO <sub>2</sub> -Cu	<i>t</i> -BuOH:H <sub>2</sub> O(1:3)/r.t.	3	91	62
5	<b>Cu/MWCNT-GAA@Fe<sub>3</sub>O<sub>4</sub></b>	<b>H<sub>2</sub>O/50°C</b>	<b>1</b>	<b>99</b>	<b>This work</b>

To optimize the required amount of catalyst the synthesis of 1-benzyl-4-phenyl-1H-1,2,3- triazole was performed as a model reaction and the results are summarized in Table 3. Optimization of amount of catalyst showed that the 0.400 mol% of catalyst is needed to provide the best results. The optimum conditions were 0.400 mol% Cu/MWCNT-GAA@Fe<sub>3</sub>O<sub>4</sub> and H<sub>2</sub>O as the solvent for click reaction.

**Table 3.** Effect of amount of catalyst and temperature on click reaction<sup>a</sup>

Entry	Amount of catalyst (mol%)	Temperature	Yield <sup>b</sup> (%)
1	None	50°C	<5
2	0.1	50°C	25
3	0.2	50°C	43
4	0.3	50°C	63
5	<b>0.4</b>	<b>50°C</b>	<b>99</b>
6	0.4	25°C	60

<sup>a</sup> Reaction conditions: phenylacetylene (1 mmol), benzyl bromide (1 mmol) and sodium azide (1 mmol), water (5 ml), 1 h. <sup>b</sup> Isolated yield

One of the advantages of this active heterogeneous nanomagnetic catalyst is its ability to perform as a recyclable reaction medium. To evaluate the level of reusability and stability of the catalyst, we examined click experiments with phenylacetylene, benzyl bromide and sodium azide using the recycled Cu/MWCNT-GAA@Fe<sub>3</sub>O<sub>4</sub> catalyst under the mentioned conditions (Table 1, Entry 1). After the carrying out of the first reaction, the catalyst was concentrated on the sidewall of the reaction flask using an external magnet and the catalyst washing with acetone (2 × 5 mL) and subsequently dried at 60 °C and then reused. Only minor decreases in the reaction yield were observed after four repetitive cycles for this reaction (Fig. 5a). The decanted solution was collected for determination of copper leaching. The Cu leaching of the catalyst was determined to be 0.002 wt% based on the FAAS analysis. Fig. 5b showed FT-IR spectra of recovered catalyst after four run, no significant differences were observed in the peaks before and after using the nanocatalyst. Also, TEM image proved the presence of the Cu NPs. As it is shown in Fig. 5c the structure of Cu/MWCNT-GAA@Fe<sub>3</sub>O<sub>4</sub> nanocomposite has remained quite stable and there is no evidence of any agglomeration or defect on MWCNT structure.



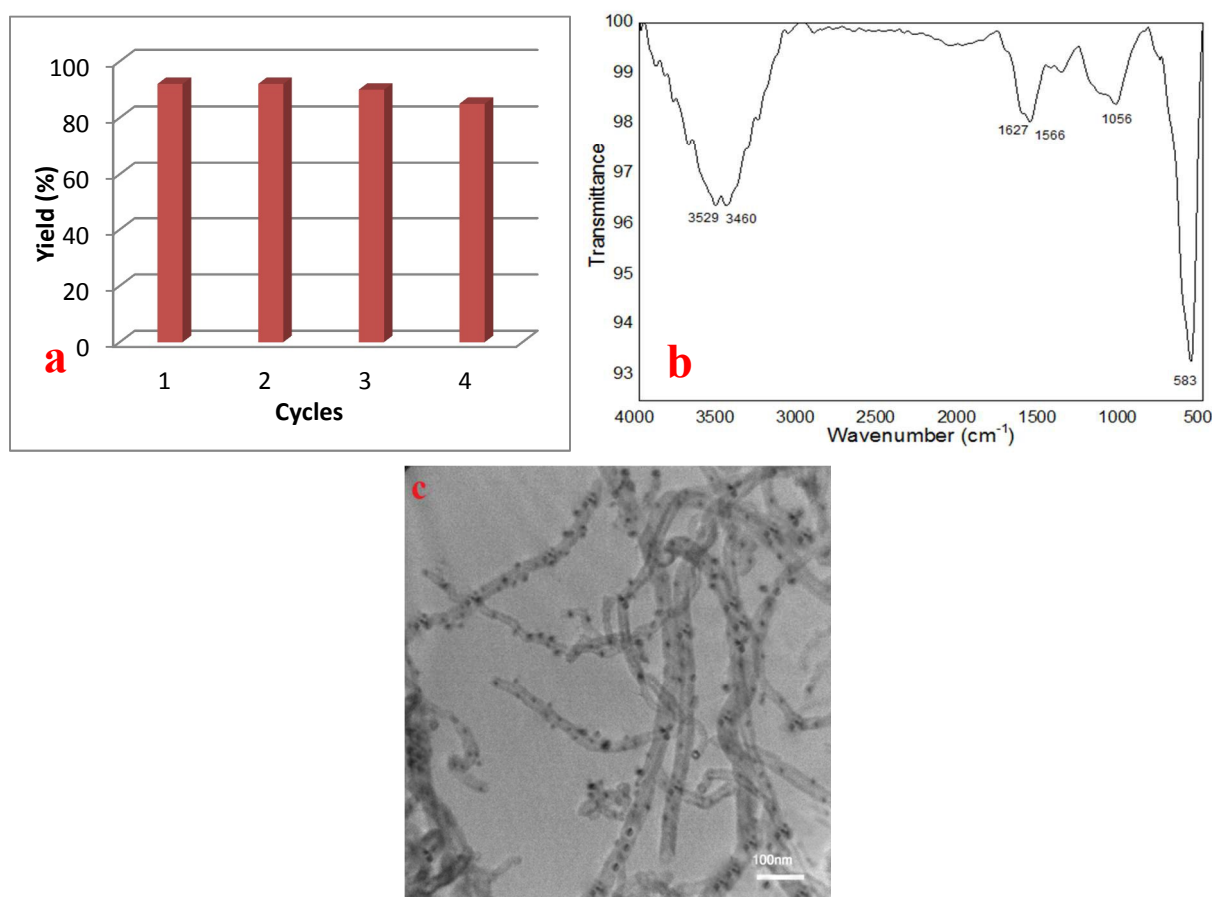
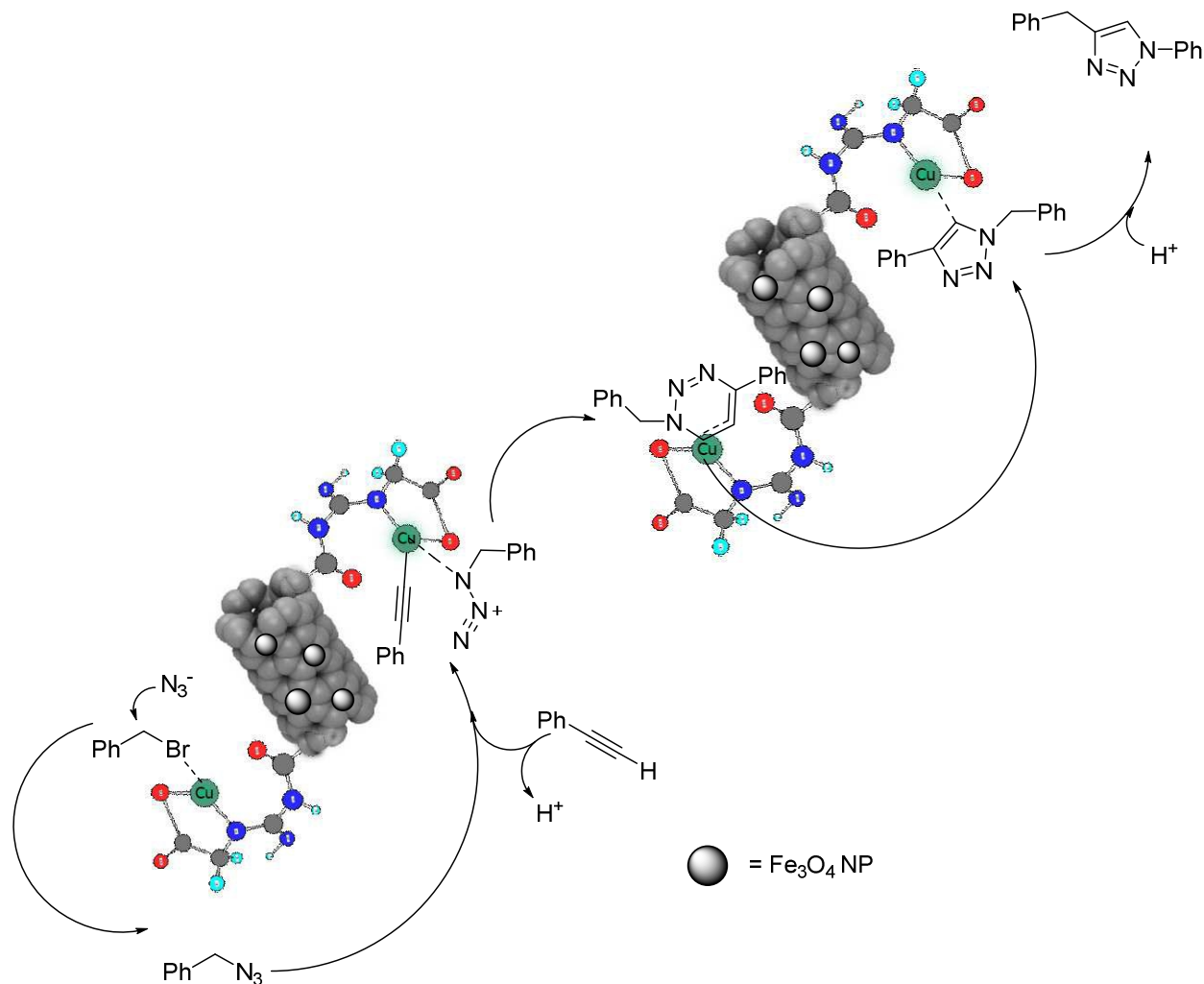


**Fig. 5** (a) Reusability of the catalyst for the click reaction, (b) FT-IR spectra, (c) TEM image of recovered catalyst after 4<sup>th</sup> run

Mechanistically, we proposed that the reaction might proceed on the surface of the Cu/MWCNT-GAA@Fe<sub>3</sub>O<sub>4</sub> nanocatalyst by initial dipole-dipole and ionic interaction between the catalyst surface and reagents. In the first step, benzyl azide was formed through the nucleophilic substitution reaction of azide ion with benzyl bromide. Afterward, the supported Cu NPs can readily insert into terminal alkynes for polarization of the terminal triple bonds. This phenomenon was catalysed the cycloaddition reaction of phenyl azide and alkyne for producing the target molecule (Scheme 3).



**Scheme 3.** Proposed mechanism of click reaction with Cu/MWCNT-GAA@Fe<sub>3</sub>O<sub>4</sub> nanocomposite

Along with a growing demand on multi-task catalysts for a wide range of reactions and because of the click reaction has been carried out successfully using the prepared nanocatalyst, therefore the usability of these catalytic system has been examined for the one of the considerable condensation reactions toward the synthesis of bis(indolyl)methanes. Interestingly, it was found that Cu/MWCNT-GAA@Fe<sub>3</sub>O<sub>4</sub> was proved to be an efficient catalyst not only for producing 1,2,3-triazoles, but also has a great catalytic role in the synthesis of bis(indolyl)methanes using water as a solvent. Results of this reaction summarized in Table 4.

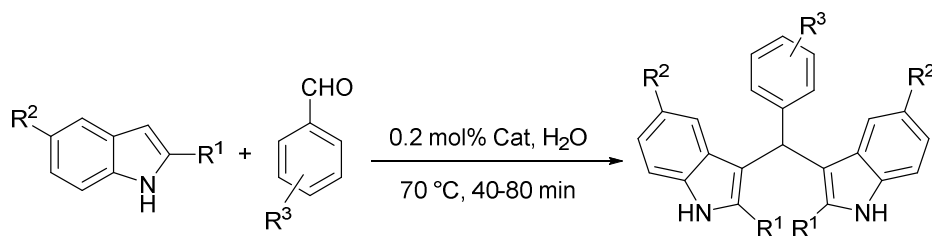


**Table 4.** Synthesis of bis(indolyl)methanes catalyzed by Cu/MWCNT-GAA@Fe<sub>3</sub>O<sub>4</sub> using indole derivation and various benzaldehyde in water

Entry	R <sup>1</sup>	R <sup>2</sup>	R <sup>3</sup>	Yield <sup>a</sup> (%)	M.p. (°C) (L)
1	H	H	H	88	150-152 (148–149) <sup>33</sup>
2	H	H	4-NO <sub>2</sub>	96	215-218 (216–217) <sup>33</sup>
3	H	H	4-Cl	94	78-79 (75–78) <sup>33</sup>
4	H	H	4-CH <sub>3</sub>	86	94-97 (94–95) <sup>33</sup>
5	H	H	2-propargyl	84	177-178
6	Me	H	H	92	188-190 (185–188) <sup>33</sup>
7	Me	H	2-Cl	90	216-219 (220–221) <sup>33</sup>
8	H	Br	4-NO <sub>2</sub>	86	297-300 (294–297) <sup>33</sup>

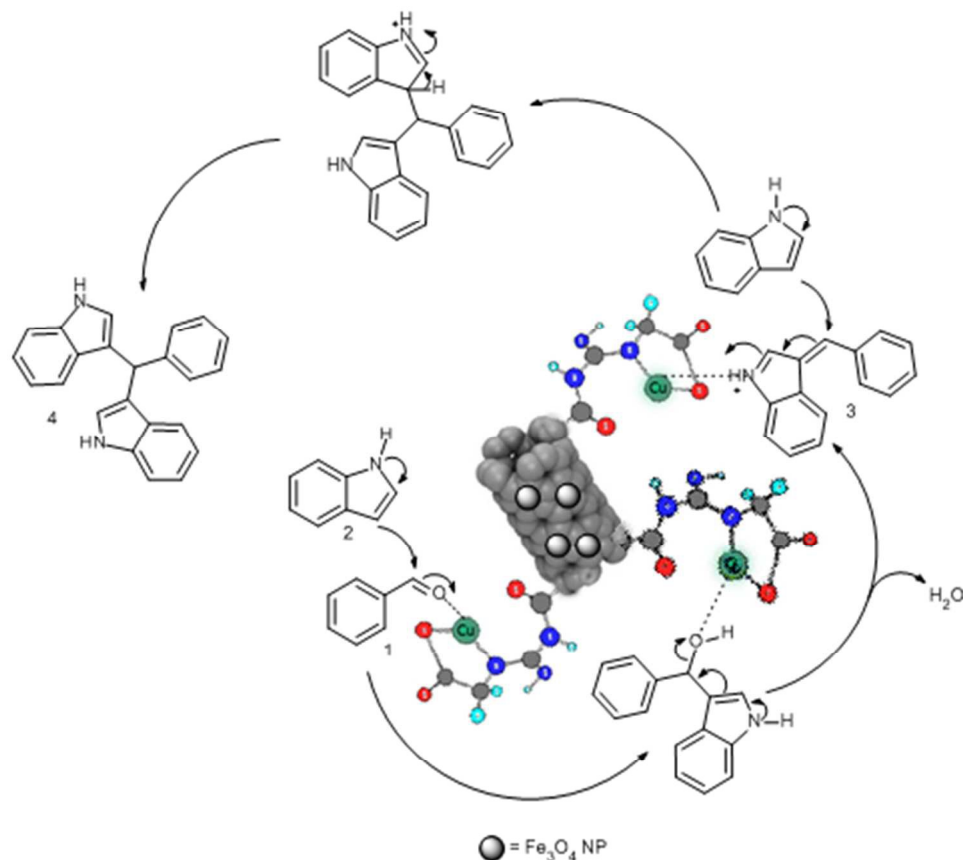
<sup>a</sup>Isolated yield

The efficiency of various Cu catalysts<sup>63-66</sup> was examined for synthesis of bis(indolyl) methanes, and the results are shown in Table 5. Among these Cu catalysts, Cu-modified MWCNT-GAA@Fe<sub>3</sub>O<sub>4</sub> is superior, compared to literature data, with respect to the catalyst, solvent and yield. The results showed that Cu/MWCNT-GAA@Fe<sub>3</sub>O<sub>4</sub> nanocomposite can acts as a powerful catalyst for activation of carbonyl functional groups and consequently have an interesting role in the synthesis of bis(indolyl)methanes.

**Table 5.** Comparison of literature catalysts and this work for the synthesis of bis(indolyl) methanes

Entry	Catalyst	Solvent	Time (min)	Yield (%)	Ref
1	CuBr <sub>2</sub>	CH <sub>3</sub> CN	15	93	63
2	Cu <sub>1.5</sub> PMo <sub>12</sub> O <sub>40</sub>	ionic liquid	10	83	64
3	Cu(BF <sub>4</sub> ) <sub>2</sub> ·SiO <sub>2</sub>	CH <sub>2</sub> Cl <sub>2</sub>	75	92	65
4	Cu(NO <sub>3</sub> ) <sub>3</sub> ·3H <sub>2</sub> O	CH <sub>3</sub> CN	330	82	66
5	Cu/MWCNT-GAA@Fe <sub>3</sub> O <sub>4</sub>	water	40	96	<b>This work</b>

A possible mechanism for the reaction between indole and benzaldehyde derivatives in the presence of Cu/MWCNT-GAA@Fe<sub>3</sub>O<sub>4</sub> has been shown in Scheme 4. It seems that the Cu/MWCNT-GAA@Fe<sub>3</sub>O<sub>4</sub> nanocomposite activates the benzaldehyde 1 toward electrophilic attack of indole 2 to generate indolyl carbinol which further converts to azafulvenium intermediate 3. The intermediate 3 can undergo further addition with a second indole molecule to produce bis(indolyl) methanes 4.



**Scheme 4.** Plausible reaction mechanism for the formation of bis(indolyl) methanes by Cu/MWCNT-GAA@ $\text{Fe}_3\text{O}_4$  nanocomposite

## Conclusions

In conclusion, we have introduced Cu-modified MWCNT-GAA@ $\text{Fe}_3\text{O}_4$  nanocatalyst for the first time which can expeditiously acts as a catalyst in organic synthesis. With this attractive and novel catalyst, we have developed a simple and efficient method for the 1,3-dipolar cycloaddition of terminal alkynes with azides and bis(indolyl)methanes in water as a green solvent. The advantages of applied of this catalyst are short times, easy of handling, high atom economy and simple work-up also all the products were obtained in good to excellent yield and the catalyst was reusable up to four times without much loss in catalytic activity. Our multi-task heterogeneous metallic-based catalyst was able to be involved in at least two consecutive reactions having a different mechanism and represents the merger of two ubiquitous green chemistry themes: magnetic nanoparticles as easily recoverable catalysts and aqueous medium for organic reactions. These results thus broaden the scope of this catalyst in the other organic chemistry.

## Spectral data for new derivatives of 1,2,3-triazoles

1-(4-Nitrobenzyl)-4-(4-(trifluoromethyl)phenyl)-1H-1,2,3-triazole (Table 1, Entry 6). White powder; m.p.: 215-218 °C,  $^1\text{H}$  NMR (300 MHz,  $\text{CDCl}_3$ )  $\delta$  (ppm) 5.74 (2H, s), 7.47-7.50 (2H, m), 7.68-7.71 (2H, m), 7.84 (1H, s), 7.94-7.96 (2H, m), 8.26-8.29 (2H, m);  $^{13}\text{C}$  NMR (75 MHz,  $\text{CDCl}_3$ )  $\delta$  (ppm) 53.1, 118.1, 120.0, 120.5, 121.8, 124.9, 125.2, 127.7, 132.5, 140.1, 147.2.

1-(3-Iodobenzyl)-4-p-tolyl-1H-1,2,3-triazole (Table 1, Entry 7). white powder; m.p. 178-181 °C;  $^1\text{H}$  NMR (300 MHz,  $\text{CDCl}_3$ )  $\delta$  (ppm) 2.38 (3H, s), 5.51 (2H, s), 7.09-7.14 (1H, m), 7.22-7.27 (3H, m), 7.62-7.72 (5H, m);  $^{13}\text{C}$  NMR (75 MHz,  $\text{CDCl}_3$ )  $\delta$  (ppm) 21.3, 53.2, 94.7, 118.85, 119.25, 119.58, 125.63, 127.51, 129.50, 129.63, 130.77, 136.80, 136.97, 137.86, 138.16, 148.49, 158.53.

#### Spectral data for new derivative of bis(indolyl)methane

3-((1H-Indol-3-yl)(2-(prop-2-ynyloxy)phenyl)methyl)-1H-indole (Table 2, Entry 5). Dark red powder; m.p. 177-178 °C;  $^1\text{H}$  NMR (300 MHz,  $\text{DMSO}-d_6$ )  $\delta$  (ppm) 3.58 (1H, s), 4.87 (2H, s), 6.23 (1H, s), 6.76-6.86 (4H, m), 7.13-7.36 (10H, m), 10.79 (2H, brs);  $^{13}\text{C}$  NMR (75 MHz,  $\text{DMSO}-d_6$ )  $\delta$  (ppm) 31.9, 56.2, 78.5, 80.1, 111.8, 113.8, 118.0, 118.5, 119.4, 121.3, 123.9, 124.0, 127.1, 127.2, 129.8, 133.7, 136.8, 137.0, 154.6; Anal. Calcd. (%) for  $\text{C}_{26}\text{H}_{20}\text{N}_2\text{O}$ : C, 82.95; H, 5.35; N, 7.44. Found: C, 82.90; H, 5.42; N, 7.21.

#### Acknowledgements

We gratefully acknowledge financial support from the Iran National Science Foundation (INSF), the Research Council of Shahid Beheshti University and Catalyst Center of Excellence (CCE) at Shahid Beheshti University.

#### Appendix A. Supplementary data

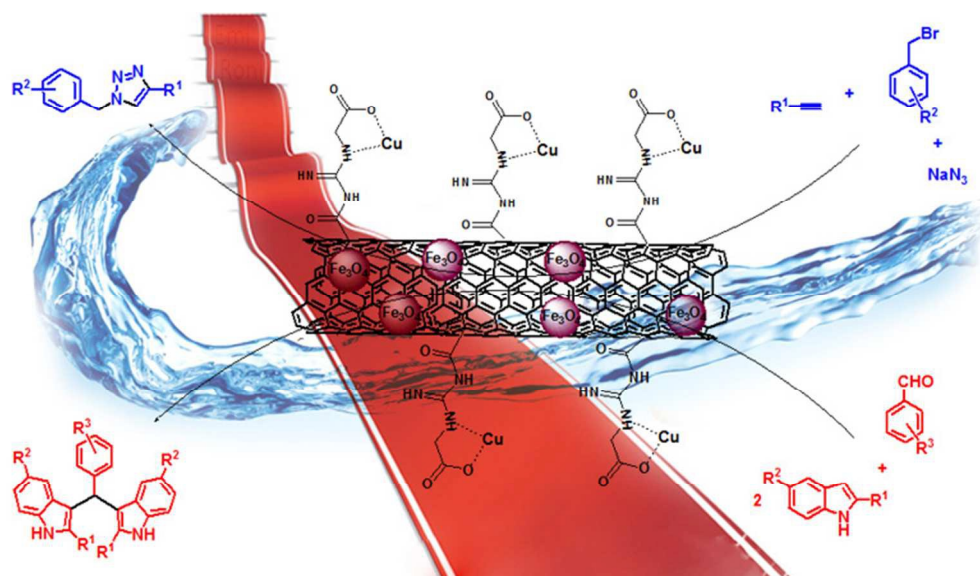
Supplementary data associated with this article can be found, in the online version.

#### References

1. Y. Yan, J. Miao, Z. Yang, F.-X. Xiao, H. B. Yang, B. Liu and Y. Yang, *Chem. Soc. Rev.*, 2015, **44**, 3295-3346.
2. D. R. Dreyer, H. P. Jia and C. W. Bielawski, *Angew. Chem.*, 2010, **122**, 6965-6968.
3. J. Pyun, *Angew. Chem. Int. Ed.*, 2011, **50**, 46-48.
4. S. Liao, F. Peng, H. Yu and H. Wang, *Appl. Catal., A*, 2014, **478**, 1-8.
5. M. B. Gawande, A. K. Rath, I. D. Nogueira, R. S. Varma and P. S. Branco, *Green Chem.*, 2013, **15**, 1895-1899.
6. I. Kalinina, Y. F. Al-Hadeethi, E. Bekyarova, C. Zhao, Q. Wang, X. Zhang, A. Al-Zahrani, F. Al-Agel, F. Al-Marzouki and R. C. Haddon, *Mater. Lett.*, 2015, **142**, 312-316.
7. Z. Liu, X. Fu, S. Tang, Y. Cheng, L. Zhu, L. Xing, J. Wang and L. Xue, *Catal. Commun.*, 2014, **56**, 1-4.
8. A. Ishibashi, Y. Yamaguchi, H. Murakami and N. Nakashima, *Chem. Phys. Lett.*, 2006, **419**, 574-577.
9. A. Satake, Y. Miyajima and Y. Kobuke, *Chem. Mater.*, 2005, **17**, 716-724.
10. L. Yang, B. Yang, D. Zeng, D. Wang, Y. Wang and L.-M. Zhang, *Carbohydr. Polym.*, 2011, **85**, 845-853.
11. R. Afshari, S. Mazinani and M. Abdouss, *NANO*, 2015, **10**, 1550010.
12. M. B. Gawande, P. S. Branco and R. S. Varma, *Chem. Soc. Rev.*, 2013, **42**, 3371-3393.
13. R. N. Baig and R. S. Varma, *Green Chem.*, 2013, **15**, 398-417.
14. J. Andrez, G. Bozoklu, G. Nocton, J. Pécaut, R. Scopelliti, L. Dubois and M. Mazzanti, *Chem. Eur. J.*, 2015, **21**, 15188-15200.
15. Q.-Z. Yang, A. Kermagoret, M. Agostinho, O. Siri and P. Braunstein, *Organomet.*, 2006, **25**, 5518-5527.
16. J. L. de Miranda and J. Felcman, *Polyhedron*, 2003, **22**, 225-233.
17. J. Ila, A. Mühl and S. Stöckler-Ipsiroglu, *Clin. Chim. Acta*, 2000, **290**, 179-188.
18. M. Kuroda, *Nephron*, 1993, **65**, 605-611.
19. J. Verhelst, J. Berwaerts, B. Marescau, R. Abs, H. Neels, C. Mahler and P. De Deyn, *Metabolism*, 1997, **46**, 1063-1067.
20. R. Osman and H. Basch, *J. Am. Chem. Soc.*, 1984, **106**, 5710-5714.
21. J. F. Lutz, *Angew. Chem. Int. Ed.*, 2007, **46**, 1018-1025.
22. H. C. Kolb, M. Finn and K. B. Sharpless, *Angew. Chem. Int. Ed.*, 2001, **40**, 2004-2021.
23. V. D. Bock, H. Hiemstra and J. H. Van Maarseveen, *Eur. J. Org. Chem.*, 2006, **2006**, 51-68.
24. S. Röper, H. C. Kolb, W. Jahnke and D. Erlanson, *Click chemistry for drug discovery*, Wiley-VCH Verlag GmbH & Co. KGaA: Weinheim, Germany, 2006.
25. H. Nandivada, H. Y. Chen, L. Bondarenko and J. Lahann, *Angew. Chem. Int. Ed.*, 2006, **45**, 3360-3363.
26. F. Alonso, Y. Moglie, G. Radivoy and M. Yus, *Org. Biomol. Chem.*, 2011, **9**, 6385-6395.
27. J. Kim, J. Park and K. Park, *Chem. Commun.*, 2010, **46**, 439-441.
28. M. Bandini and A. Eichholzer, *Angew. Chem. Int. Ed.*, 2009, **48**, 9608-9644.
29. M. G. Russell, R. J. Baker, L. Barden, M. S. Beer, L. Bristow, H. B. Broughton, M. Knowles, G. McAllister, S. Patel and J. L. Castro, *J. Med. Chem.*, 2001, **44**, 3881-3895.

30. D. Maciejewska, M. Rasztańska, I. Wolska, E. Anuszevska and B. Gruber, *Eur. J. Med. Chem.*, 2009, **44**, 4136-4147.
31. D. Kumar, V. Arun, N. Maruthi Kumar, G. Acosta, B. Noel and K. Shah, *ChemMedChem*, 2012, **7**, 1915-1920.
32. M. Shiri, M. A. Zolfigol, H. G. Kruger and Z. Tanbakouchian, *Chem. Rev.*, 2009, **110**, 2250-2293.
33. A. Z. Halimehjani, S. E. Hooshmand and E. V. Shamiri, *RSC Adv.*, 2015, **5**, 21772-21777.
34. D. Sun, G. Jiang, Z. Xie and Z. Le, *Chin. J. Chem.*, 2015, **33**, 409-412.
35. Z. Xiang, Z. Liu, X. Chen, Q. Wu and X. Lin, *Amino acids*, 2013, **45**, 937-945.
36. D. Chandam, A. Mulik, P. Patil, S. Jagdale, D. Patil, S. Sankpal and M. Deshmukh, *J. Mol. Liq.*, 2015, **207**, 14-20.
37. M. Mahyari, M. S. Laeini and A. Shaabani, *Chem. Commun.*, 2014, **50**, 7855-7857.
38. A. Shaabani and Z. Hezarkhani, *Cellulose*, 2015, **22**, 3027-3046.
39. A. Shaabani, S. Keshipour, M. Hamidzad and S. Shaabani, *J. Mol. Catal. A: Chem.*, 2014, **395**, 494-499.
40. S. Keshipour and A. Shaabani, *Appl. Organomet. Chem.*, 2014, **28**, 116-119.
41. A. Shaabani and M. Mahyari, *J. Mater. Chem. A*, 2013, **1**, 9303-9311.
42. M. Mahyari and A. Shaabani, *Appl. Catal., A*, 2014, **469**, 524-531.
43. M. Mahyari, A. Shaabani and Y. Bide, *RSC Adv*, 2013, **3**, 22509-22517.
44. A. Shaabani, M. Mahyari and F. Hajishaabani, *Res. Chem. Intermed.*, 2014, **40**, 2799-2810.
45. M. Mahyari and A. Shaabani, *J. Mater. Chem. A*, 2014, **2**, 16652-16659.
46. Y. Liu, P. Liu, Z. Su, F. Li and F. Wen, *Appl. Surf. Sci.*, 2008, **255**, 2020-2025.
47. J. Felcman and J. L. d. Miranda, *J. Brazil. Chem. Soc.*, 1997, **8**, 575-580.
48. N. Arsalani, H. Fattahi and M. Nazarpour, *Express Polym. Lett.*, 2010, **4**, 329-338.
49. M. Salavati-Niasari and F. Davar, *Mater. Lett.*, 2009, **63**, 441-443.
50. S. Sun and H. Zeng, *J. Am. Chem. Soc.*, 2002, **124**, 8204-8205.
51. V. V. Rostovtsev, L. G. Green, V. V. Fokin and K. B. Sharpless, *Angew. Chem. Int. Ed.*, 2002, **41**, 2596-2599.
52. M. S. Costa, N. Boechat, E. A. Rangel, F. d. C. Da Silva, A. M. De Souza, C. R. Rodrigues, H. C. Castro, I. N. Junior, M. C. S. Lourenço and S. M. Wardell, *Bioorg. Med. Chem.*, 2006, **14**, 8644-8653.
53. H. Nandivada, X. Jiang and J. Lahann, *Adv. Mater.*, 2007, **19**, 2197-2208.
54. G. C. Tron, T. Pirali, R. A. Billington, P. L. Canonico, G. Sorba and A. A. Genazzani, *Med. Res. Rev.*, 2008, **28**, 278-308.
55. A. Shaabani, M. Seyyedhamzeh, N. Ganji, M. H. Sangachin and M. Armaghan, *Mol. Divers.*, 2015, **19**, 709-715.
56. A. Shaabani, E. Soleimani and H. R. Khavasi, *Tetrahedron Lett.*, 2007, **48**, 4743-4747.
57. A. Shaabani, A. Sarvary, S. Ghasemi, A. H. Rezayan, R. Ghadari and S. W. Ng, *Green Chem.*, 2011, **13**, 582-585.
58. A. Z. Halimehjani, S. E. Hooshmand and E. V. Shamiri, *Tetrahedron Lett.*, 2014, **55**, 5454-5457.
59. N. Joshi and S. Banerjee, *Tetrahedron Lett.*, 2015, **56**, 4163-4169.
60. R. U. Islam, A. Taher, M. Choudhary, M. J. Witcomb and K. Mallick, *Dalton Trans.*, 2015, **44**, 1341-1349.
61. R. Hudson, C.-J. Li and A. Moores, *Green Chem.*, 2012, **14**, 622-624.
62. P. Diz, P. Pernas, A. El Maatougui, C. R. Tubio, J. Azuaje, E. Sotelo, F. Guitián, A. Gil and A. Coelho, *Appl. Catal., A*, 2015, **502**, 86-95.
63. L. P. Mo, Z. C. Ma and Z. H. Zhang, *Synth. Commun.*, 2005, **35**, 1997-2004.
64. N. Seyedi, H. Khabazzadeh and K. Saidi, *Mol. Divers.*, 2009, **13**, 337-342.
65. G. Meshram and V. D. Patil, *Synth. Commun.*, 2009, **40**, 29-38.
66. A. Nareen, R. Varala, S. R. Adapa, *J. Heterocycl. Chem.*, 2007, **44**, 983.





276x156mm (72 x 72 DPI)